

# Preparation of Porous $\text{In}_2\text{O}_3$ Powders by Ultrasonic-spray Pyrolysis Employing PMMA Microspheres Synthesized by Emulsion Polymerization and Their Gas-sensing Properties

Takeo Hyodo<sup>1,\*</sup>, Shu-ichi Furuno<sup>2</sup>, Eriko Fujii<sup>2</sup>, Matsuo Katsuhide<sup>1</sup>,  
Suguru Motokucho<sup>1</sup>, Ken Kojio<sup>1</sup> and Yasuhiro Shimizu<sup>1</sup>

<sup>1</sup>Graduate School of Engineering, <sup>2</sup>Faculty of Engineering, Nagasaki University,  
1-14 Bunkyo-machi, Nagasaki 852-8521, Japan

\*hyodo@nagasaki-u.ac.jp

## Abstract

The suspension containing polymethylmethacrylate (PMMA) microspheres was synthesized by the emulsion polymerization employing methyl methacrylate monomer, sodium lauryl sulfate as a surfactant and ammonium persulfate as an initiator, and porous  $\text{In}_2\text{O}_3$  powders (pr- $\text{In}_2\text{O}_3$ (M), M:  $\text{In}_2\text{O}_3$  source (N:  $\text{In}(\text{NO}_3)_3$ , Cl:  $\text{InCl}_3$ )) were prepared by ultrasonic-spray pyrolysis of  $\text{In}(\text{NO}_3)_3$  or  $\text{InCl}_3$  aqueous solution containing the synthesized PMMA microspheres as a template. The average diameter of the PMMA microspheres, which was measured by dynamic light scattering, was ca. 60.2 nm. The pr- $\text{In}_2\text{O}_3$ (N) powder consisted of large microspheres with well-developed spherical mesopores ( $\leq$  ca. 30 nm in diameter) and a small number of macropores (ca. 100 nm in diameter) on the spherical surface, while the pr- $\text{In}_2\text{O}_3$ (Cl) powder was composed of meso-sized particles (ca. 30 nm in diameter), respectively. On the other hand, the morphology of conventional  $\text{In}_2\text{O}_3$  powder (c- $\text{In}_2\text{O}_3$ (N)) prepared by ultrasonic-spray pyrolysis of PMMA-free  $\text{In}(\text{NO}_3)_3$  aqueous solution as a reference was roughly-spherical with a diameter of ca. 100~700 nm and the bulk was relatively dense. The  $\text{NO}_2$  response of pr- $\text{In}_2\text{O}_3$ (M) sensors was much larger than that of a c- $\text{In}_2\text{O}_3$ (N) sensor. In addition, the response and recovery speeds of the pr- $\text{In}_2\text{O}_3$ (M) sensors were faster than those of the c- $\text{In}_2\text{O}_3$ (N) sensor.

**Key words:** gas sensor, polymethylmethacrylate microsphere, emulsion polymerization, porous  $\text{In}_2\text{O}_3$  powder, ultrasonic-spray pyrolysis,  $\text{NO}_2$

## Introduction

We have already designed microstructural morphology of various gas-sensing materials with different sizes of well-developed pores, to improve their gas-sensing properties. For example, mesoporous semiconductor metal oxides with large specific surface area and small crystallites were prepared by utilizing a self-assembly of a surfactant such as *n*-cetylpyridinium chloride and a triblock copolymer such as Pluronic P-123 (BASF Corp.,  $\text{EO}_{20}\text{PO}_{80}\text{EO}_{20}$  (EO: ethylene oxide, PO: propylene oxide)) as a template, and the average diameter of their well-developed mesopores was in the range of 2~5 nm [1-5]. The treatment of the as-prepared mesoporous oxides with phosphoric acid largely improved their thermal stability at temperatures up to 600°C, while maintaining their large specific surface area and small crystallites. Therefore, the phosphoric-acid treatment enabled us to use mesoporous oxides as gas sensor materials at elevated temperatures. On the other hand,

macroporous oxides were also prepared by different preparation methods such as modified sol-gel technique [6], ultrasonic-spray pyrolysis [7-10], sputtering [11] and pulsed laser deposition [12], employing commercial PMMA microspheres (150~800 nm in diameter) as a template. Since the pore size of the macroporous oxides was  $\geq$  ca. 100 nm in diameter, the introduction of relatively-large pores improved significantly the gas diffusivity in the gas-sensing films and/or disks, and in turn the gas-sensing properties. However, we have not yet established a preparation method to prepare gas-sensing materials having well-developed middle-sized pores with a diameter of 5~100 nm. Such technique is absolutely essential for designing the nano- and micro-structures suitable for achieving well controlled gas reactivity and diffusivity in gas-sensing films and/or disks and then drastic enhancement in the gas-sensing properties.

In this study, therefore, we have attempted to synthesize PMMA microsphere templates with

a diameter of several tens nanometers by ourselves, to prepare porous  $\text{In}_2\text{O}_3$  powders having mesopores originating from the PMMA microspheres, and then to clarify the morphological properties as well as the  $\text{NO}_2$  sensing properties.

### Experimental

PMMA microspheres were prepared in distilled water ( $100 \text{ cm}^3$ ) by the ultrasonic (19.5 kHz)-assisted emulsion polymerization ( $60^\circ\text{C}$ , 50 min) employing methyl methacrylate monomer (8 g) as a polymer source, sodium lauryl sulfate (0.1 g) as a surfactant and ammonium persulfate (0.3 g) as an initiator. The particle size distribution of the PMMA microspheres obtained was measured by dynamic light scattering (DLS, Malvern instrument Ltd., HPPS).

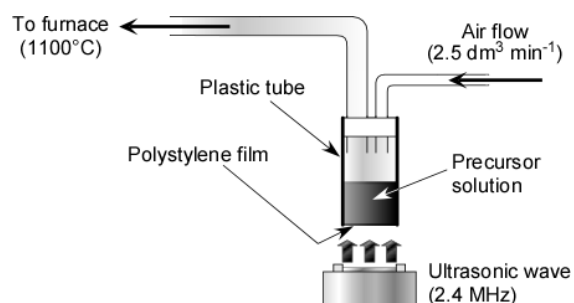


Fig. 1. Schematic drawing of a feeding system of a precursor solution atomized by ultrasonication (2.4 MHz).

To prepare the precursor solution of  $\text{In}_2\text{O}_3$ , the PMMA suspension was mixed with a 0.5 M  $\text{In}(\text{NO}_3)_3$  or  $\text{InCl}_3$  aqueous solution (suspension : solution = 37.5 : 100 in volume ratio). The mist of the precursor solution obtained was generated by ultrasonic irradiation (2.4 MHz) and then it was directly heat-treated in an electric furnace at  $1100^\circ\text{C}$  under air flowing ( $2.5 \text{ dm}^3 \text{ min}^{-1}$ ) by using a feeding system, as shown in Fig. 1. The porous powders obtained were denoted as pr- $\text{In}_2\text{O}_3$ (M) (M:  $\text{In}_2\text{O}_3$  source (N:  $\text{In}(\text{NO}_3)_3$ , Cl:  $\text{InCl}_3$ )). Conventional  $\text{In}_2\text{O}_3$  (c- $\text{In}_2\text{O}_3$ (N)) was also prepared by the similar preparation technique using PMMA-free  $\text{In}(\text{NO}_3)_3$  aqueous solution. The microstructure of all samples was observed with scanning electron microscope (SEM; JEOL Ltd., JSM-7500F or JCM-5700) and transmission electron microscope (TEM; JEOL Ltd., JEM2010). The specific surface area (SSA) and pore size distribution were measured by the Brunauer-Emmett-Teller (BET) method using a  $\text{N}_2$  adsorption isotherm (Micromeritics Instrument Corp., Tristar3000). Crystal phase was characterized by X-ray diffraction analysis (XRD; Rigaku Corp., RINT2200) using  $\text{Cu K}\alpha$

radiation (40 kV, 40 mA), and crystallite size (CS) was calculated from the (101) diffraction peak using Scherrer equation.

Thick film sensors were fabricated by the screenprinting employing the paste of each  $\text{In}_2\text{O}_3$  powder on an alumina substrate equipped with a pair of interdigitated Pt electrodes, followed by calcination at  $550^\circ\text{C}$  for 5 h. Gas response of these sensors was measured to 10 ppm  $\text{NO}_2$  balanced with air in a flow apparatus in the temperature range of  $150\sim 500^\circ\text{C}$ . The magnitude of  $\text{NO}_2$  response was defined as the ratio ( $R_g/R_a$ ) of sensor resistance after 10 min exposure to  $\text{NO}_2$  ( $R_g$ ) balanced with air to that in air ( $R_a$ ).

### Results and discussion

Relatively uniform PMMA microspheres with a diameter of less than 100 nm were easily synthesized by ultrasonic-assisted emulsion polymerization. Figure 2 shows particle size distribution measured by the DLS. It is confirmed that the average diameter of the PMMA microspheres was ca. 60.2 nm. The size of PMMA microspheres synthesized is much smaller than that of the smallest one which was employed as a template in our previous study (Soken Chem. & Eng. Co. Ltd., MP-1451, ca. 150 nm in diameter) [6-12].

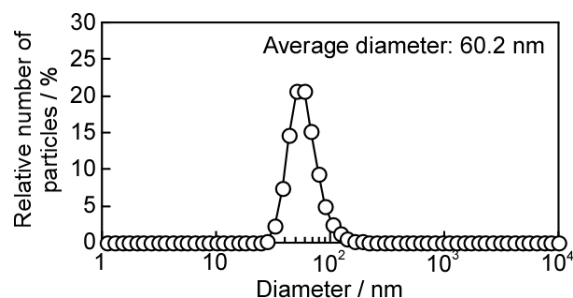


Fig. 2. Particle size distribution of PMMA microspheres.

Figures 3 and 4 shows SEM and TEM photographs of pr- $\text{In}_2\text{O}_3$ (M) powders and c- $\text{In}_2\text{O}_3$ (N) powder, respectively. Morphology of the c- $\text{In}_2\text{O}_3$ (N) powder was roughly-spherical with ca. 100~700 nm in diameter, and the TEM observation indicated that the bulk was relatively dense. In addition, SSA and CS of the c- $\text{In}_2\text{O}_3$ (N) powder was  $1.56 \text{ m}^2 \text{ g}^{-1}$  and 25.9 nm, respectively. Assuming that the density of c- $\text{In}_2\text{O}_3$ (N) crystallites is  $7.180 \text{ g cm}^{-3}$  [13] and the morphology of the crystallites is spherical, the geometric surface area which is estimated from the crystallite size calculated by the Scherrer equation (25.9 nm) is ca.  $32.1 \text{ m}^2 \text{ g}^{-1}$ . The fact that the SSA of the c- $\text{In}_2\text{O}_3$ (N) powder was much smaller than that of the geometric surface area suggests the existence

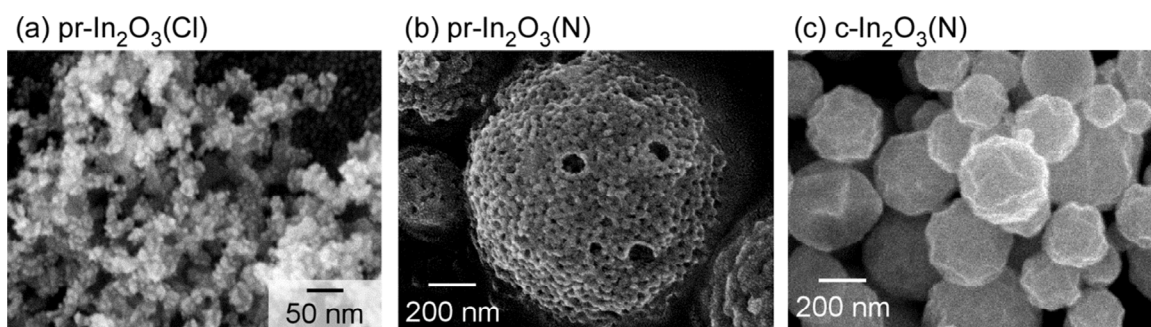


Fig. 3. SEM photographs of pr-In<sub>2</sub>O<sub>3</sub>(M) and c-In<sub>2</sub>O<sub>3</sub>(N) powders.

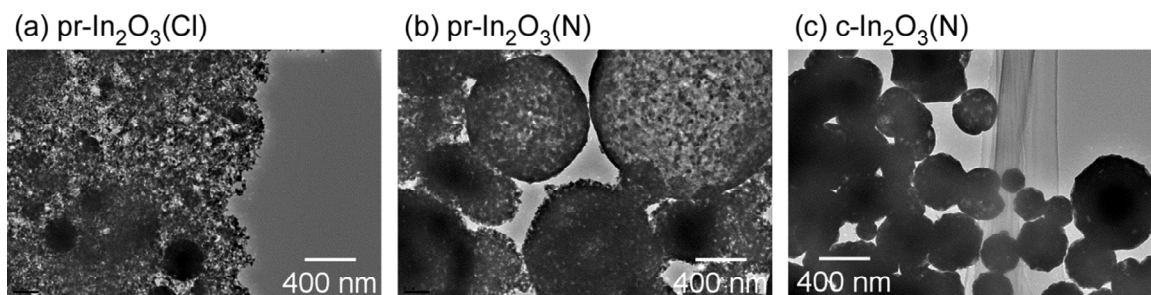


Fig. 4. TEM photographs of pr-In<sub>2</sub>O<sub>3</sub>(M) and c-In<sub>2</sub>O<sub>3</sub>(N) powders.

of several crystallites inside one particle and then dense and less pores in the particle.

pr-In<sub>2</sub>O<sub>3</sub>(N) powder consisted of large microspheres with well-developed spherical mesopores (pore diameter:  $\leq$  ca. 30 nm) and a small number of macropores (pore diameter: ca. 100 nm) on the spherical surface, as shown in Fig. 3 (b). The formation of well-developed pores in the internal region of the pr-In<sub>2</sub>O<sub>3</sub>(N) powder was also confirmed by the TEM observation (Fig. 4 (b)), but information on further detailed nanostructure was hard to be obtained. At least, these results show that the PMMA microspheres synthesized by this ultrasonic-assisted polymerization technique can be effectively utilized as a template to prepare porous gas-sensing materials. As can be expected from these morphologies, the SSA of the pr-In<sub>2</sub>O<sub>3</sub>(N) powder ( $19.1 \text{ m}^2 \text{ g}^{-1}$ ) was much larger than that of the c-In<sub>2</sub>O<sub>3</sub>(N) powder, while the CS of the pr-In<sub>2</sub>O<sub>3</sub>(N) powder (15.3 nm) was smaller than that of the c-In<sub>2</sub>O<sub>3</sub>(N) powder. On the other hand, the morphology of pr-In<sub>2</sub>O<sub>3</sub>(Cl) powder are extremely different from that of pr-In<sub>2</sub>O<sub>3</sub>(N) powder, although the difference in the preparation method was just raw chemicals (InCl<sub>3</sub> or In(NO<sub>3</sub>)<sub>3</sub>). The pr-In<sub>2</sub>O<sub>3</sub>(Cl) powder consisted of many meso-sized particles with a diameter of less than 30 nm and a few submicron-sized microspheres, as shown in Figs. 3 (a) and 4 (a). The SSA of the pr-In<sub>2</sub>O<sub>3</sub>(Cl) powder ( $30.5 \text{ m}^2 \text{ g}^{-1}$ ) was much larger than that of the pr-In<sub>2</sub>O<sub>3</sub>(N) powder, whereas the CS of the pr-In<sub>2</sub>O<sub>3</sub>(Cl) powder (17.8 nm) was slightly larger than of the pr-In<sub>2</sub>O<sub>3</sub>(N) powder.

These differences of SSA and CS values between the pr-In<sub>2</sub>O<sub>3</sub>(N) and pr-In<sub>2</sub>O<sub>3</sub>(Cl) powders may indicate that pr-In<sub>2</sub>O<sub>3</sub>(Cl) particles are rather small in size, but consisting of rather large crystallites, in comparison with pr-In<sub>2</sub>O<sub>3</sub>(N) particles (i.e., particles structuring microspheres). Detailed mechanism of the formation of different morphologies of In<sub>2</sub>O<sub>3</sub> powders is not clarified yet and is our future subject.

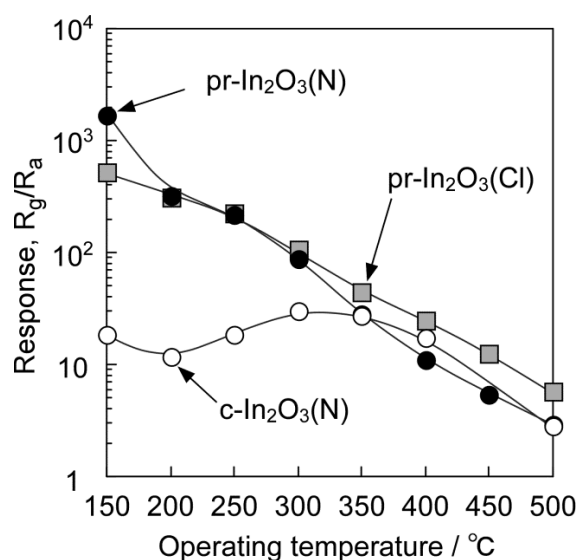


Fig. 5. Operating temperature dependence of response of pr-In<sub>2</sub>O<sub>3</sub>(M) and c-In<sub>2</sub>O<sub>3</sub>(N) sensors to 10 ppm NO<sub>2</sub> in air.

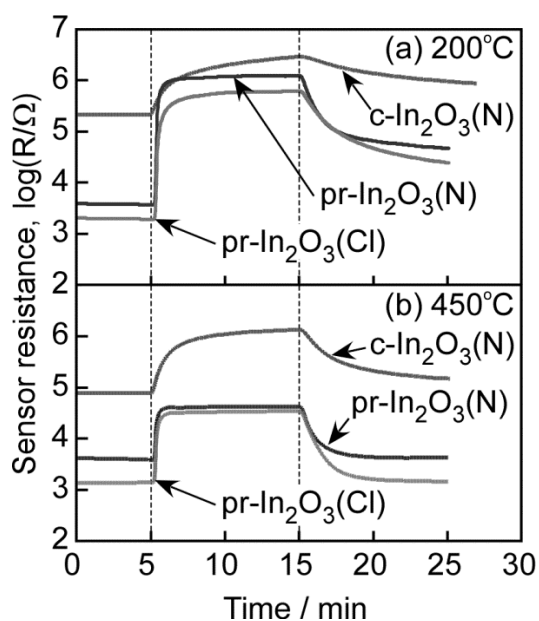


Fig. 6. Representative response transients of  $pr\text{-In}_2\text{O}_3(\text{M})$  and  $c\text{-In}_2\text{O}_3(\text{N})$  sensors to 10 ppm  $\text{NO}_2$  in air at 200 and 450°C.

Figures 5 and 6 show operating temperature dependence of response to 10 ppm  $\text{NO}_2$  and response transients to 10 ppm  $\text{NO}_2$  at 250°C and 400°C of  $pr\text{-In}_2\text{O}_3(\text{M})$  and  $c\text{-In}_2\text{O}_3(\text{N})$  sensors to in air, respectively. The magnitude of  $\text{NO}_2$  responses of the  $pr\text{-In}_2\text{O}_3(\text{M})$  sensors at 150°C was extremely large, but it decreased monotonically with an increase in the operating temperature (Fig. 5). In addition, the  $\text{NO}_2$  responses were hardly dependent on the morphological difference between  $pr\text{-In}_2\text{O}_3(\text{N})$  and  $pr\text{-In}_2\text{O}_3(\text{Cl})$ . On the other hand, the  $c\text{-In}_2\text{O}_3(\text{N})$  sensor showed the magnitude of  $\text{NO}_2$  response similar to those of the  $pr\text{-In}_2\text{O}_3(\text{M})$  sensors at higher temperatures (over 300°C), but the much lower  $\text{NO}_2$  response than those of the  $pr\text{-In}_2\text{O}_3(\text{M})$  sensors at lower temperature (below 300°C). In addition, response and recovery speeds of the  $pr\text{-In}_2\text{O}_3(\text{M})$  sensors were much faster than those of the  $c\text{-In}_2\text{O}_3(\text{N})$  sensor in the whole temperature range studied (Fig. 6). Thus, it is confirmed that the addition of PMMA microspheres to the precursor solution and then the introduction of porous structure in the oxide powder were effective in improving the  $\text{NO}_2$  response especially at low temperatures and the response and recovery speeds over the whole temperature range. The results of the present study predicts the improvement of gas sensing performance of various semiconductor metal oxides other than  $\text{In}_2\text{O}_3$ , by the introduction of nano- and micro-porous structure into the powder. Such an approach is now under investigation.

## References

- [1] T. Hyodo, N. Nishida, Y. Shimizu, M. Egashira, *Sensors and Actuators B*83, 209-215 (2002); doi: 10.1016/S0925-4005(01)01042-5
- [2] G. S. Devi, T. Hyodo, Y. Shimizu, M. Egashira, *Sensors and Actuators B*87, 122-129 (2002); doi: 10.1016/S0925-4005(02)00228-9
- [3] Y. Shimizu, A. Jono, T. Hyodo, M. Egashira, *Sensors and Actuators B*108, 56-61 (2005); doi: 10.1016/j.snb.2004.10.047
- [4] T. Hyodo, K. Murayama, Y. Shimizu, M. Egashira, *Rare Metal Materials and Engineering*35, Suppl. 3, 455-458 (2006); doi: CNKI:SUN:COSE.0.2006-S3-141
- [5] T. Tsumura, T. Hyodo, Y. Shimizu, *Sensor Letters*9, 646-650 (2011); doi: 10.1166/sl.2011.1582
- [6] T. Hyodo, K. Sasahara, Y. Shimizu, M. Egashira, *Sensors and Actuators B*106, 580-590 (2005); doi: 10.1016/j.snb.2004.07.024
- [7] K. Hieda, T. Hyodo, Y. Shimizu, M. Egashira, *Sensors and Actuators B* 133, 144-150 (2008); doi: 10.1016/j.snb.2008.02.002
- [8] M. Hashimoto, H. Inoue, T. Hyodo, Y. Shimizu, M. Egashira, *Sensor Letters* 6, 887-890 (2008); doi: 10.1166/sl.2008.524
- [9] A. Anaraki Firooz, T. Hyodo, A. Reza Mahjoub, A. Ali Khodadadi, Y. Shimizu, *Sensors and Actuators B*147, 554-560 (2010); doi: 10.1016/j.snb.2010.03.021
- [10] T. Hyodo, H. Inoue, H. Motomura, K. Matsuo, T. Hashishin, J. Tamaki, Y. Shimizu, M. Egashira, *Sensors and Actuators B*150, 264-273 (2010); doi: 10.1016/j.snb.2010.09.002
- [11] T. Hyodo, A. Bieberle-Hütter, J. L. Hertz, H. L. Tuller, *Journal of Electroceramics*17, 695-699 (2006); doi: 10.1007/s10832-006-4987-3
- [12] I.-D. Kim, A. Rothschild, T. Hyodo, H. L. Tuller, *Nano Letters* 6, 193-198 (2006); doi: 10.1021/nl051965p
- [13] M. J. O'Neil (Ed.), *The Merck Index*, 14th ed., Merck & Co., Inc., p. 860 (2006).